JOURNAL OF VOLCANOLOGY AND SEISMOLOGY, 2025, No. 1, pp. 57–77

LABAZNOE PORPHYRY ORE-MAGMATIC SYSTEM (OMOLON CRATON TERRAIN, NORTH-EAST OF RUSSIA): AGE, MINERALOGY OF MINERALIZATION AND MINERAL THERMOBAROMETRY OF ORE-HOSTING GRANITOIDS OF THE VIKTORINSKY COMPLEX

© 2025 V. Yu. Solov'ev[a, *], V. V. Priymenko[a, **], G. O. Polzunenkov[a, *], M. I. Fomina[a], T. I. Mikhalitsyna[a], A. M. Gagieva[a], V. B. Khubanov[b], P. P. Kolegov[a], and V. V. Akinin[a]**

[a] *North-Eastern Complex Research Institute named after N. A. Shilo, Far Eastern Branch of the Russian Academy of Sciences, Magadan, Russia*
[b] *Dobretsov Geological Institute SB RAS, Ulan-Ude, Russia*
**e-mail: solovev@neisri.ru*
***e-mail: priymenkovladimir@gmail.com*
****e-mail: gennadiy_mag@mail.ru*

Received June 29,2024
Revised October 07, 2024
Accepted October 28, 2024

Abstract. New data are presented on the age (U–Pb, LA-SF-ICP-MS: 86 ± 1 Ma) of quartz monzodiorites of the Viktorinsky complex of the Kongin magmatic zone of the Omolon cratonic terrane. The Labaznoye ore occurrence, bearing veinlet-stockwork sulfide-quartz and vein polymetallic mineralization, is localized within the intrusive-dome uplift, in the central part of which a stock of monzodiorites of the Viktorinsky complex is exposed. The petrographic and geochemical characteristics and mineral thermobarometry of the ore-hosting quartz monzodiorites are presented. The mineralogy of the ores is characterized and an estimate of the isotopic age (K–Ar: 82 ± 4 Ma) of sericite crystallization from the near-vein contact with the monzodiorite intrusion are characterized. Based on geological relationships and isotope-geochronological data, a paragenetic relationship was established between molybdenum-porphyry mineralization and the stage of Late Cretaceous magmatism – the intrusion of granitoid bodies of the Viktorinsky complex. The stages of formation of paragenetic mineral associations were reconstructed in the sequence magnetite-quartz, molybdenite-quartz, sulfide-quartz; the hypogene stage ends with a polymetallic mineralization. The isotope dating materials of ores and ore-hosting granitoids in the study region indicate a Late Cretaceous (Coniacian-Campanian) age of porphyry ore-magmatic systems of the Kongin magmatic zone.

Keywords: *porphyry ore-magmatic system, isotopic age, mineralogy, petrography, thermobarometry*

DOI: 10.31857/S02030306250104e2

INTRODUCTION

Within the Omolon cratonic terrane (CT), traditionally called the Omolon Massif, several molybdenum-porphyry ore occurrences are known: Khrustalnoe, Vechernee, Shlikhovoe, Zakharenko (Fig. 1), which are confined to Late Cretaceous granitoid intrusions of the Viktorinsky complex [Goryachev et al., 2017; Glukhov et al., 2021].

Granitoid bodies (predominantly sills, small multiphase stocks, less commonly dikes and individual relatively large massifs), composed of porphyritic monzonites, granodiorites, quartz diorites, granosyenites, rarely gabbro of the early phase, are spatially combined with outcrops of volcanogenic-sedimentary, effusive and subvolcanic formations of the Kongin andesite-rhyolite complex, forming unified volcano-tectonic structures. Volcanogenic formations of the Kongin complex are attributed to the Late Cretaceous based on findings of floristic remains in the volcanogenic-sedimentary deposits of the Kongin Formation (LOS-200, Shevchenko, Simakov, 1999)[1]. The close spatial association of granitoid intrusions of the Viktorinsky complex with volcanogenic formations of the Kongin complex, their interrelationships and belonging to a single structure, similar petro- and geochemical properties served as the basis for combining them into the Late Cretaceous Kongin volcano-plutonic association (LOS-200). Volcanogenic formations of the Konginskiy complex and associated intrusions of the Viktorinskiy complex can be traced as a chain of isolated volcanic structures, forming the linear Kongin magmatic zone (MZ). The Kongin MZ is located in the central part of the Omolon CT, extending in a submeridional direction for 200–250 km along the Konginskiy deep fault, and is bounded by the zones of Omkuchanskiy and Tebaninskiy deep faults from the north and south (see Fig. 1). According to the opinion of most researchers, the Kongin MZ is a linear, orthogonal to the general strike, structural element of the Okhotsk-Chukotka volcanic belt (OChVB).

The metallogenic potential of the Kongin MZ has a high assessment [Goryachev et al., 2017]; numerous deposits and ore occurrences of gold-silver, silver-polymetallic, gold-rare metal, and copper-molybdenum-porphyry mineralization are known here (Bodroe, Kustiki/Sedoe, Zakharenko, Dzhelty, etc.). At the same time, the lack of information about the composition and age of the ore mineralization and the magmatism that produces it, and the small proportion of modern analytical data generate a discussion about the formational affiliation and type of ore formation for a number of ore objects. These include the Labaznoe ore occurrence, which is considered as a gold-polysulfide type of gold-silver formation associated with the Middle

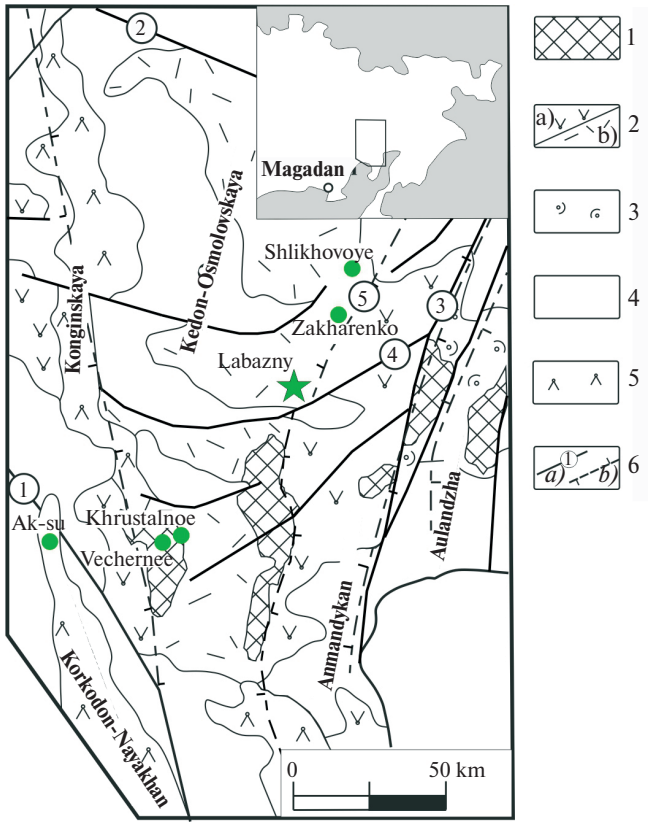

Fig. 1. Geological-tectonic scheme of the Omolon cratonic terrane, based on materials from [Egorov et al., 2001; Terekhov et al., 1984] with additions.
1 – outcrops of the Pre-Riphean crystalline basement; 2, 3 – Middle Paleozoic Kedon basalt-andesite-rhyolite complex: 2 – volcanogenic deposits of basic to intermediate (*a*), acidic (*b*) composition, 3 – volcanogenic-molasse deposits of Late Devonian – Early Carboniferous; 4 – Carboniferous-Early Cretaceous sedimentary and volcanogenic-sedimentary deposits; 5 – OChVB and its feathering Korkodon-Nayakhan and Kongin magmatic zones; 6 – *a* – faults (1 – Tebaninsky, 2 – Omkuchansky, 3 – Verkhne-Omolonsky, 4 – Nekuchansky, 5 – Koargychansky), *b* – boundaries of structural-formational zones: Aulandzha, Anmandykan, Kedon-Omolon. Green circles and stars indicate copper-molybdenum-porphyry ore occurrences paragenetically associated with Late Cretaceous granitoids.

[1] *Shevchenko V.M., Simakov K.V.* Legend of the Omolon series of the State Geological Map of the Russian Federation, scale 1:200,000. Second edition. Magadan: SevVostNITsMIS, 1999. 173 p.

Paleozoic (Early Devonian – Early Carboniferous) stage of magmatism of the Omolon CT [Kuznetsov et al., 2001], or – as a fully manifested porphyry ore-magmatic system corresponding to the Late Cretaceous stage of magmatic activity of the OChVB [Glukhov et al., 2021].

This publication presents new data on the age of granitoid magmatism and associated ore mineralization of the Labaznoe object; *P-T* conditions of crystallization of the magmatic melt have been reconstructed; materials of a comprehensive study of ore mineralogy are provided; a conclusion is made about the genetic type of ore formation.

RESEARCH METHODS

The work is based on the author's collection of samples gathered during fieldwork in 2019. Petrographic and mineralogical studies were carried out by the authors using an Axioplan Imagin microscope with the PETRO software package [Polzunenkov, Kondratiev, 2023]. Chemical compositions of rock-forming and ore minerals, totaling 957 measurements from 10 samples, were determined using a Camebax microanalyzer with an X-Max energy-dispersive spectrometer (analysts V.Yu. Solovyov, E.M. Goryacheva). Measurements were conducted with an accelerating voltage of 20 kV, magnification over ×400, and spectrum accumulation time of 30 s. Optimization for quantitative calculations was performed using chemically pure copper every 1.5–2.0 h. Certified natural [Jarosewich et al., 1980] and synthetic materials were used as standards. The detection limit for elements was 0.3 wt. %, with an electron beam diameter of 3–4 μm.

U–Pb dating of zircon was carried out using the LA-SF-ICP-MS method, based on a single-collector magnetic sector mass spectrometer with inductively coupled plasma Element XR and a UP-213 laser ablation system at the Shared Research Facility "Geospektr" of the N.L. Dobretsov Geological Institute SB RAS (Ulan-Ude). Sample preparation and analysis were performed according to standard procedures following [Khabanov et al., 2016]. Zircon standard 91500 [Wiedenbeck et al., 1995] was used as an external standard. Mass spectrometric analysis data were processed using "Glitter" [Van Achterbergh et al., 2001; Griffin et al., 2008] and "IsoplotR" [Vermeesch, 2018] software. The problem of assessing discordance in two independent systems that exists for Cretaceous zircon crystals – low amount of ^{207}Pb in crystals and large error in determining $^{207}Pb/^{206}Pb$ isotopic age, was solved using $^{206}Pb/^{238}U$ isotopic age corrected for ^{207}Pb [Williams, 1998].

K-Ar isotope dating of sericite, isolated from the near-vein contact in quartz monzodiorites, was conducted at the Laboratory of Petrology and Isotope Geochronology of SVKNII FEB RAS (Magadan) on a mass spectrometer MI-1201IG (analyst V.V. Lavrenko). Potassium concentrations were measured on an atomic absorption spectrometer AAS-1 (analyst Ya.S. Ignatenko) with an error of less than 1%. The age calculations used constants recommended by the XXI session of the Commission for Determining Absolute Age: $1_k = 0.581 \times 10^{-10}$ year^{-1}; $1_b = 4.962 \times \times 10^{-10}$ year^{-1}; isotope abundance: ^{39}K – 93.26; ^{40}K – 0.01167; ^{41}K – 6.73 at.%; isotopic ratio of atmospheric argon $^{40}Ar/^{36}Ar = 295.5$ [Steiger, Jager, 1977].

GEOLOGICAL STRUCTURE OF THE LABAZNOE ORE FIELD

The Labaznoe ore occurrence is located near the eastern boundary of the Kongin MZ, near the concealed Koargychan deep fault of submeridional strike, which separates the Kedon-Omolon and Anmandykan structural-formational zones (according to [Egorov et al., 2002]) of the Omolon CT. In the central part of the ore area, outcrops of quartz syenites and monzodiorites of the Late Cretaceous Viktorinsky complex and subvolcanic bodies of rhyolites of the Middle Paleozoic Kedon complex have been identified (Fig. 2). Along the periphery of the intrusive bodies, basalt dykes (presumably of Cretaceous age) with a northeastern strike are distributed. The ore-hosting formations are represented by stratified volcanogenic strata of the Kedon series of Middle Paleozoic age, in the structure of which here (according to V.N. Pankov,

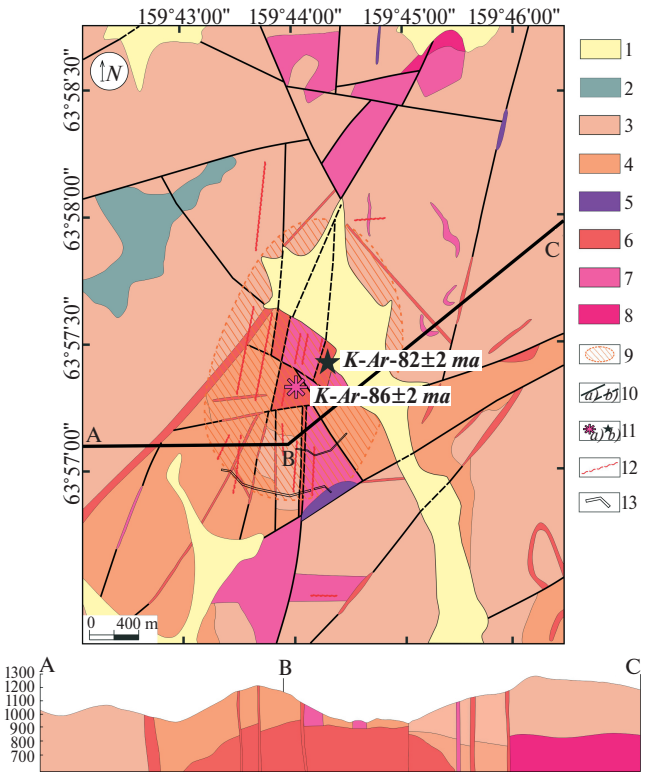

Fig. 2. Geological map and cross-section along the A–B–C line of the Labaznoe ore field, according to (V.N. Shamin, 1987; V.N. Pankov, 1990) with additions. 1 – loose Quaternary alluvial deposits; 2–4 – Middle Paleozoic volcanics of the Kedon series: 2 – trachyandesites of the Sniper Formation ***(C_1sn)***, 3 – ignimbrites and rhyodacite tuffs of the Lednikskaya Formation ***(D_3ld)***, 4 – andesites, andesite-basalts and andesite-dacites of the Gruntovskaya Formation ***($D_{1-2}grt$)***; 5 – Late Cretaceous basalt dikes; 6 – Late Cretaceous intrusions of granitoids of the Viktorinsky complex; 7 – subvolcanic bodies of rhyolites of the Kedon complex of Middle Paleozoic age; 8 – outcrops of the Pre-Riphean crystalline basement; 9 – stockwork with sulfide-quartz veinlets; 10 – established faults (*a*), inferred (*b*); 11 – sampling sites for isotope dating by methods: U–Pb (a), K–Ar (*b*); 12 – zones of oriented veinlets; 13 – trenches.

1990)[2]: andesites, andesibasalts and daciandesites of *the Gruntovskaya sequence* ($D_{1-2}grt$) and volcanogenic-sedimentary formations, ignimbrites, lavas and tuffs (predominantly of acidic composition) of *the Lednikskaya sequence* (D_3ld). Trachyandesites of the *Snaiperskaya sequence* (C_1sn)

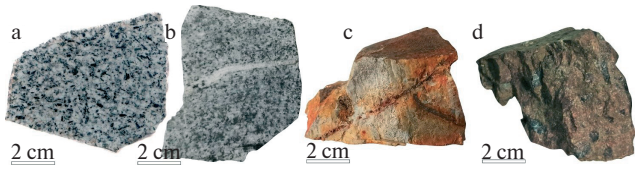

Fig. 3. Ore-hosting rocks of the Labaznoe ore field. a, b – quartz monzodiorite of the Viktorinsky complex; c – rhyolite of the Kedon complex; d – dacite ignimbrite of the Kedon series.

lie unconformably on the ignimbrites of the Lednikskaya sequence, which are well traced in the relief and armor the steep peaks of small volcanic structures. In the contact zones, the volcanics of the Lednikskaya and Snaiperskaya sequences are transformed into sericite-quartz phyllisites with thin veinlets and disseminated pyrite, chalcopyrite, and molybdenite. The most recent magmatic formations include granitoids of the Late Cretaceous Viktorinskiy complex (Fig. 3a, Fig. 3b), which form small stocks with an area of about 5 km^2 (according to magnetic survey results, taking into account the unexposed part of the dome[3]). The formation of the Labaznensk mineralization, represented by a sulfide-quartz stockwork and sulfide-quartz veins, is associated with this stage.

PETROGRAPHIC COMPOSITION OF GRANITOIDS

The Viktorinsky complex within the Labaznoe ore field is represented by stocks of dense biotite-amphibole quartz monzodiorites, from light gray to dark gray in color, with a porphyritic structure, medium-grained groundmass, and massive texture. According to the content of rock-forming oxides, the analyzed granitoids belong to quartz monzodiorites [Petrographic..., 2008] (Table 1).

[2] *Pankov V.N.* Report on the results of prospecting works at the "Labazny" object in the area of sheets P-57-8-A-b-2, 4; P-57-8-B-a, b; P-57-8-B-v-2; P-57-8-B-g-1, 2 (Labazny prospecting team). Evensk: SEGRE, 1990. Book 1. 261 p., Book 2. 228 p.

[3] *Shamin V.N., Kramarev S.P., Tedeev T.V. et al.* Report on the group geological survey and prospecting for deposits at a scale of 1:50,000 in the upper reaches of the Omolon River, in the basin of the Birkacan, Kubaki and other rivers (sheets P-57-8-A; P-57-9-A,B; P-57-8-V,G; P-57-9-V; P-57-20-A,B; P-57-21-A) for 1983–1987. Birkacan team. Seimchan, SGRE, 1987. Book 1. 335 p., Book 2. 299 p.

Table 1. Chemical composition of quartz monzodiorites from the Labazny ore field

Element	Sample	
	LBUPb 1_2	LBUPb 3_4*
SiO_2	62.41	62.32
TiO_2	0.58	0.47
Al_2O_3	18.38	17.08
$Fe_2O_{3total.}$	6.22	7.03
CaO	6.44	5.16
MgO	2.03	1.87
MnO	0.15	0.12
K_2O	2.24	3.05
Na_2O	3.64	2.82
P_2O_5	0.22	0.19
PPP	0.93	1.4
Total	103.35	100.11

Note. * – according to [Glukhov et al., 2022].

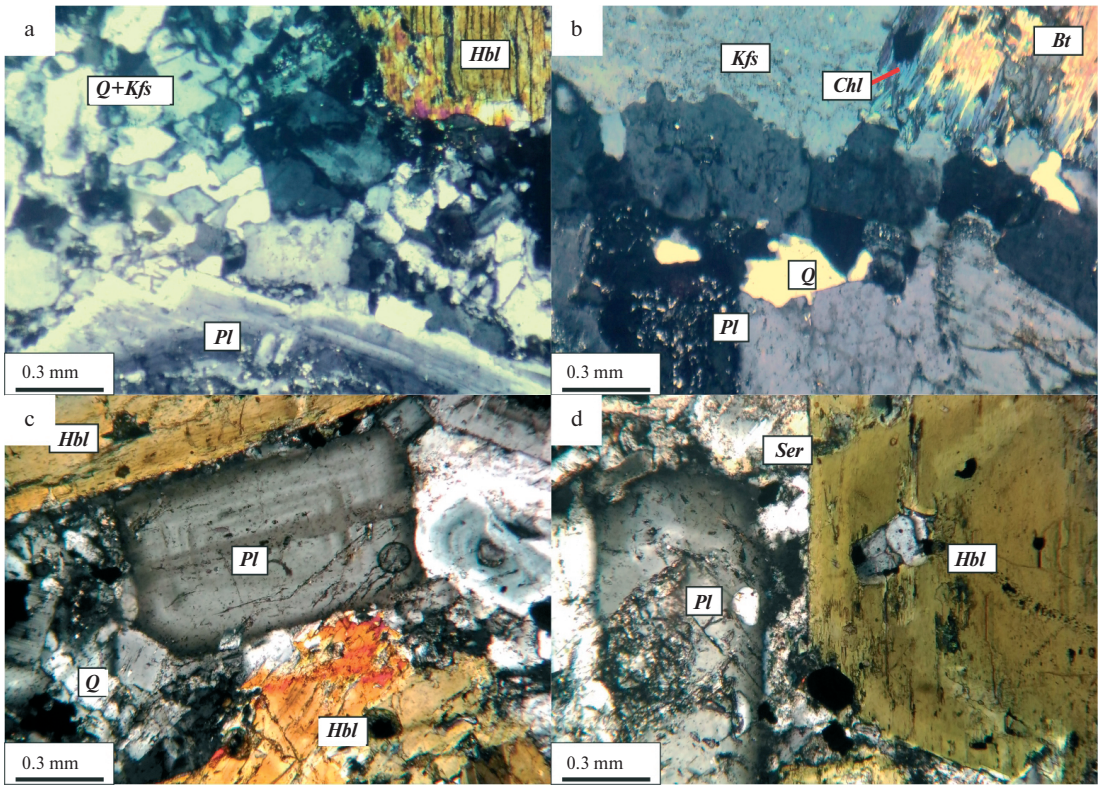

Fig. 4. Microphotographs of thin sections of quartz monzodiorites of the Viktorinsky complex of the Labaznoe ore field. Crossed nicols.
a, b – sample LBUPb 1_2, c, d – sample LBUPb 3_4. Here and further in the text, mineral designations are given according to [Laurence N. Warr., 2021].

Secondary alterations are represented by sericitization and weak silicification. The mineral composition (averaged) of quartz monzodiorites: plagioclase – 55%; amphibole – 15%; potassium feldspar – up to 10%, biotite – up to 15%, and quartz – up to 15%; accessory minerals include zircon and apatite.

The bulk of the rock consists of an allotriomorphic-grained quartz-feldspar aggregate (filling interstices between porphyritic segregations), prismatic grains of finely twinned plagioclase, and rare flakes of light mica; the grain size of the rock groundmass does not exceed 0.3 mm (Fig. 4a).

About 20% of the rock volume consists of porphyritic (0.5 to 3 mm in diameter) tabular and elongated-prismatic grains of plagioclase, hornblende, and biotite.

Porphyritic grains of plagioclase (andesine-labradorite, An_{50-65}) often have normal (direct) zonal structure – central parts correspond to labradorite ($An_{50-66(58)}$), less commonly bytownite ($An_{87-90(88.5)}$) and andesine ($An_{34-41(38)}$), marginal parts – to andesine ($An_{30-48(38)}$), less commonly labradorite ($An_{51-60(53)}$), in isolated cases oligoclase ($An_{20-28(24)}$) (Fig. 5). The central parts of plagioclase grains are saussuritized; the development of sericite along microcracks is noted.

Amphibole is represented by idiomorphic indistinctly zonal prismatic grains (up to 3 mm) of calcium hornblende – magnesian hastingsite; meanwhile, the marginal parts of the grains are often composed of magnesian hornblende and tschermakite (see Fig. 5a, 5b), which are unevenly replaced by biotite and chlorite with rims of magnetite and ilmenite. Poikilitic inclusions of quartz are noted in porphyritic grains of hornblende and plagioclase.

Biotite forms scaly and lamellar grains (up to 2 mm), often with corroded edges; it is replaced by chlorite along cleavage planes and grain edges (up to 60% of the grain area).

GEOCHEMICAL CHARACTERISTICS OF GRANITOIDS

Quartz monzodiorites of the Labaznoe ore field (samples LBUPb 1_2, LBUPb 3_4) are

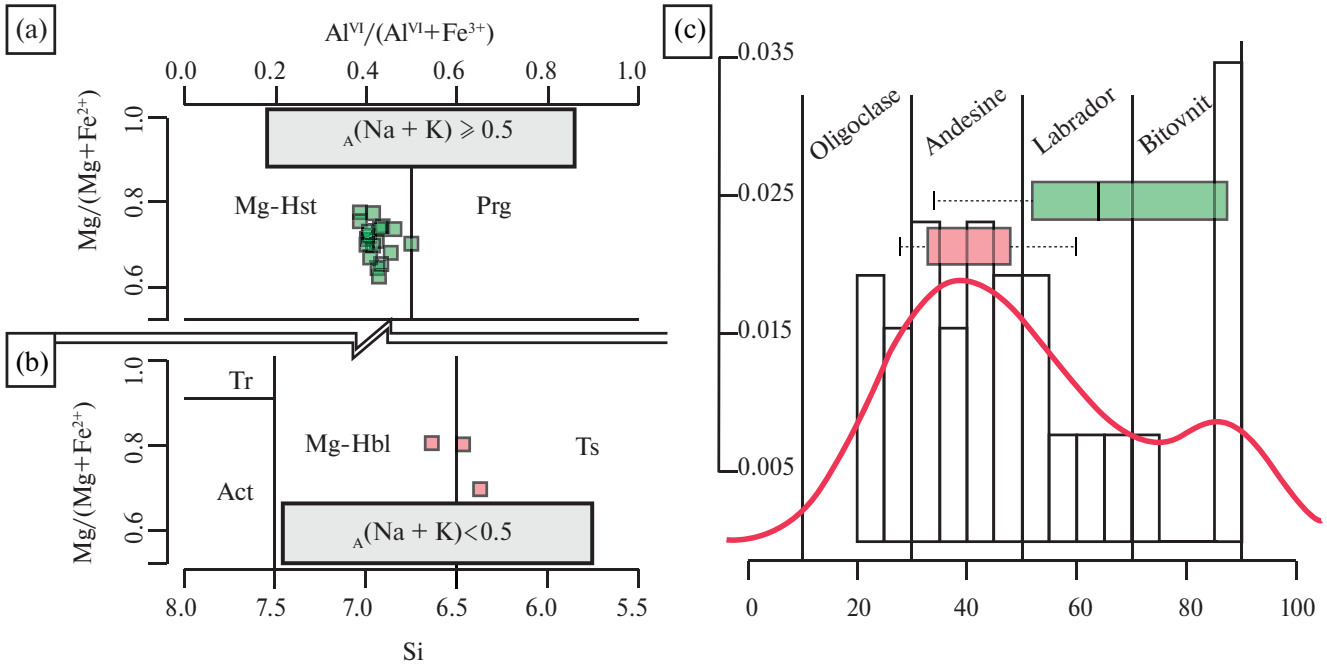

Fig. 5. Compositions of amphiboles (a, b) and plagioclases (c) of quartz monzodiorites of the Viktorinsky complex on classification diagrams [Leake et al., 1997].
Colors: green — central parts of crystals, pink – edge parts of crystals. Prg – pargasite, Mg-Hst – magnesiohastingsite, Tr – tremolite, Act – actinolite, Mg–Hbl – magnesiohornblende, Ts – tschermakite.

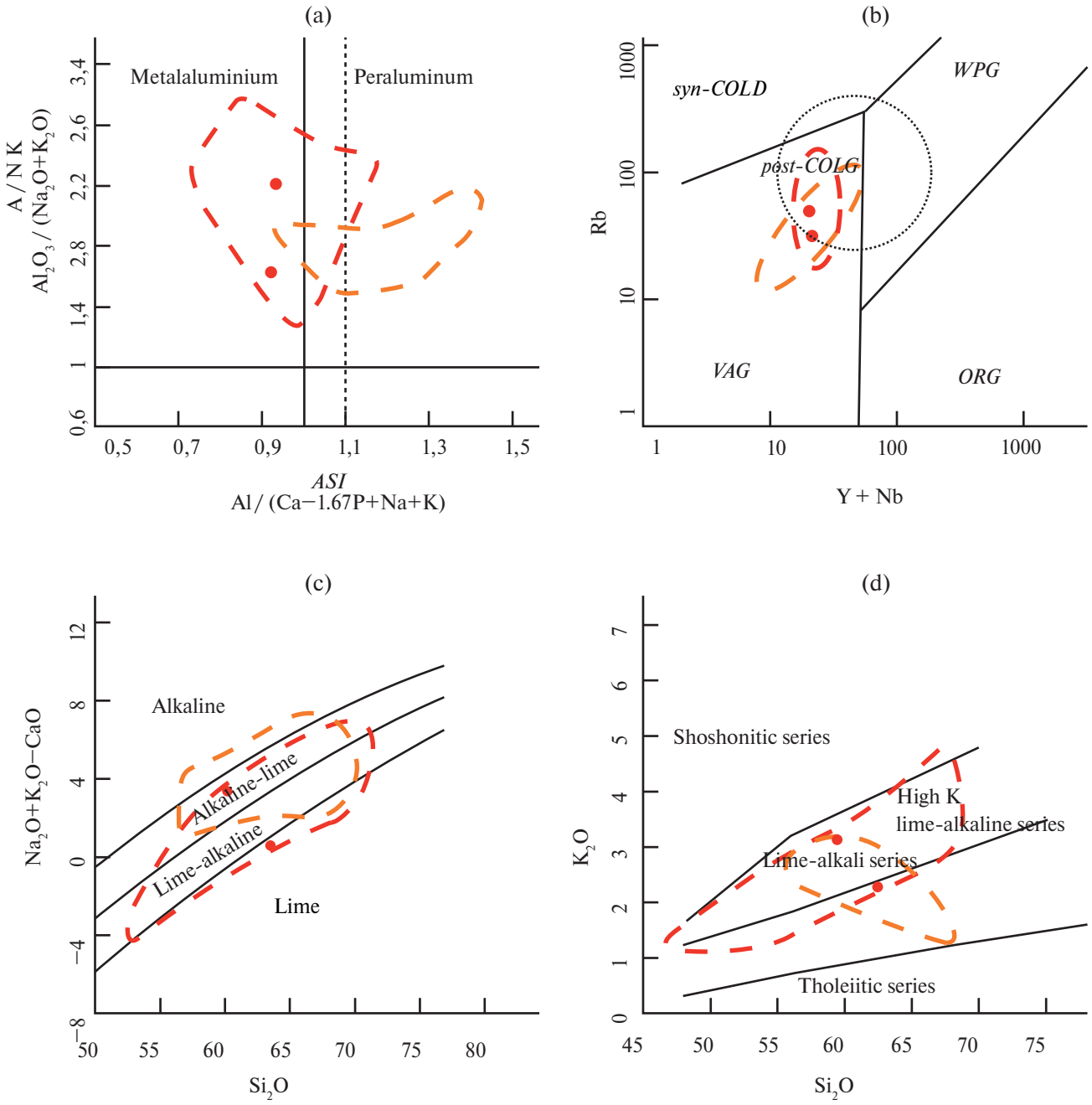

Fig. 6. Composition points of quartz monzodiorites of the Viktorinsky complex of the Labaznoe ore occurrence (red dots) on discrimination diagrams.
a – (A/NK)/ASI [Frost et al., 2001], b – Rb/Y + Nb (Pearce et al., 1984), c – $(Na_2O + K_2O – CaO)/SiO_2$ [Frost et al., 2001], d – K_2O/SiO_2 [Peccerillo and Teylor, 1976]. Composition fields on Pearce diagram – geodynamic settings: syn-COLD – collisional, post-COLD – post-collisional, WPG – within-plate, VAG – volcanic arc, ORG – ocean ridge. Dashed line – composition field contours: red – granitoids of the Viktorinsky complex of the Kongin MZ of the Omolon CT, and the Penzhin segment of the OChVB, according to [Glukhov et al., 2022, Shatova, Seregin 2023], orange – granitoids of the Early Cretaceous Namyndykan complex of the Namyndykan-Molandzhin zone of the Omolon CT, according to [Shatova, Seregin, 2023].

characterized by low loss on ignition values (LOI = 0.93–1.4 wt. %), indicating insignificant secondary alterations (see Table 1).

According to the position of figurative points on classification diagrams (Fig. 6c, 6d), the rocks are characterized as metaluminous

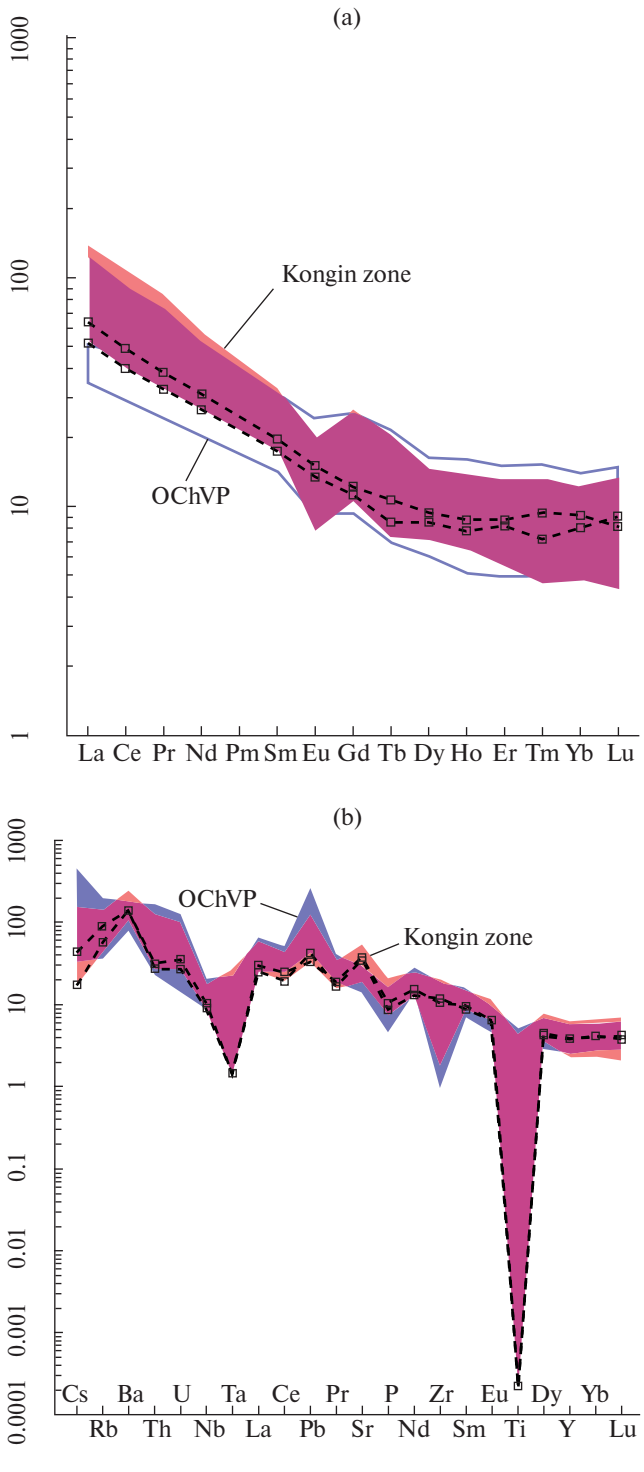

Fig. 7. Distribution curves of trace elements in quartz monzodiorites of the Viktorinsky complex of the Labaznoe ore occurrence (a – normalized to chondrite [Boyton, 1984]; b – normalized to primitive mantle [Donough, Sun, 1995]).
The colored areas show the distribution of trace elements in Cretaceous granitoids of the Viktorinsky complex (Kongin MZ – blue color) and the Garmandin complex (OChVB – orange), according to [Akinin, Miller, 2011; Glukhov et al., 2022].

I-type granitoids of magnesian ($FeO_t/(FeO_t$ + + MgO) <0.78 wt. %) and high-potassium calc-alkaline series.

Granitoids of the Victorian complex, established within the ore sites of the Kongin MZ – Labazny, Zakharenko, Sedoy, Dzhelty, belong to high-alumina, normal and moderately alkaline potassium-sodium type rocks [Glukhov et al., 2022]. Quartz monzodiorites of the Labaznoe ore field are characterized by elevated contents (relative to clarke) of As, Ba, Co, Cu, Ga, Mo, Mn, Sr, Te, Tl, V; significant enrichment in REE is noted (concentration coefficient from 4.16 to 13.75); they are enriched in light REE relative to heavy ones ($(La/Yb)_N$ = 6.5–7.1) and large ion lithophile elements (LILE: Ba, U and Pb); depleted in high field strength elements incompatible with the melt (HFSE: Nb, Ta and Ti) (Fig. 7). On the discrimination diagram of J. Pearce [Pearce et al., 1984], quartz monzodiorites are comparable to granitoids of volcanic arcs (see Fig. 6b).

MINERAL THERMOBAROMETRY OF QUARTZ MONZODIORITES

The formation conditions of quartz monzodiorites at the early magmatic stage were assessed based on the compositions of amphibole and plagioclase (thermobarometer: Hbl–melt [Putirka, 2016]; barometer: Al–in–Hbl [Mutch et al., 2016]; thermometer: Hbl–Pl [Powell, Holland, 1994]) (Table 2). The pressure and temperature parameters of the late magmatic stage were estimated using the barometer [Yang, 2017] and thermometer [Duan et al., 2021] based on the bulk composition of intermediate and acidic magmas.

Thermometer calibration is traditionally performed based on the SiO content. $_2$ content in rocks – T_{SiO2} (°C) = $-14.16 \cdot SiO_2 + 1723$ [Duan et al., 2021]; however, the authors believe that the temperature calculated in this way can only be considered for comparison, as granitoids do not represent a pure melt.

Empirical barometer of X. Yang [Yang, 2017]: $P_{(Mpa)} = -0.2426 \cdot Q^3 + 26.392 \cdot Q^2 - 980.74 \cdot Q +$ + 12 563 – relies on the normative mineral composition of granitoids. The amount of water

Table 2. Representative compositions of amphiboles from quartz monzodiorites (sample LBUPb 1_2)

Position	Center		Edge – 1		Edge – 2	
Oxides, wt. %						
SiO_2	39.98	41.81	42.28	42.19	44.89	44.12
TiO_2	2.06	1.85	2.06	2.00	2.03	2.02
Al_2O_3	13.46	12.22	11.71	11.79	8.67	9.61
*Fe_2O_3	6.30	6.69	6.28	6.95	7.80	7.19
*FeO	9.93	10.47	8.73	7.89	6.10	6.62
MgO	10.95	10.93	12.49	12.67	13.80	13.64
CaO	11.60	11.36	11.73	11.58	11.23	11.43
MnO	0.35	0.39	0.38	0.44	0.86	0.60
Na_2O	2.28	2.02	2.13	2.20	1.53	1.74
K_2O	0.78	1.03	0.67	0.65	0.65	0.52
*H_2O	1.97	1.99	2.00	2.00	2.01	2.00
Total	99.66	100.76	100.46	100.36	99.57	99.50
Formula coefficients						
T – position						
Si	5.970	6.175	6.204	6.185	6.564	6.462
Al (IV)	2.030	1.825	1.796	1.815	1.436	1.538
M1-M3 – position						
Al (VI)	0.339	0.302	0.229	0.222	0.058	0.121
Ti	0.231	0.206	0.227	0.221	0.223	0.223
Fe^{3+}	0.708	0.744	0.693	0.767	0.858	0.793
Mg	2.438	2.407	2.732	2.769	3.008	2.978
Fe^{2+}	1.240	1.293	1.071	0.967	0.746	0.811
Mn	0.044	0.049	0.047	0.055	0.107	0.074
M4 – position						
Ca	1.856	1.798	1.844	1.819	1.759	1.794
Na	0.144	0.202	0.156	0.181	0.241	0.206
A – position						
Na	0.516	0.376	0.450	0.444	0.193	0.288
K	0.149	0.194	0.125	0.122	0.121	0.097
Classification	Mg-Hst	Mg-Hst	Mg-Hst	Mg-Hst	Mg-Hbl	Ts
Calculated parameters						
[1] T (°C)	856	967	814	828	814	810
[2] P (kbar)	6.9	5.7	5.3	5.3	3.2	3.8
[3] Wt% H_2O_{melt}	7.5	6.5	6.4	6.4	4.9	5.6
[3] DNNO	0.1	0.11	0.48	0.56	1.15	1.01

Note. Calculated values, according to [Hora et al., 2001]; [1] – thermometer, according to [Holland, Blundy, 1994]; [2] – barometer, according to [Mutch et al., 2016]; [3] – hydrometer and oximeter, according to [Ridolfi et al., 2010]; Mg-Hst - magnesiohastingsite, Mg–Hbl – magnesian hornblende, Ts – tschermakite.

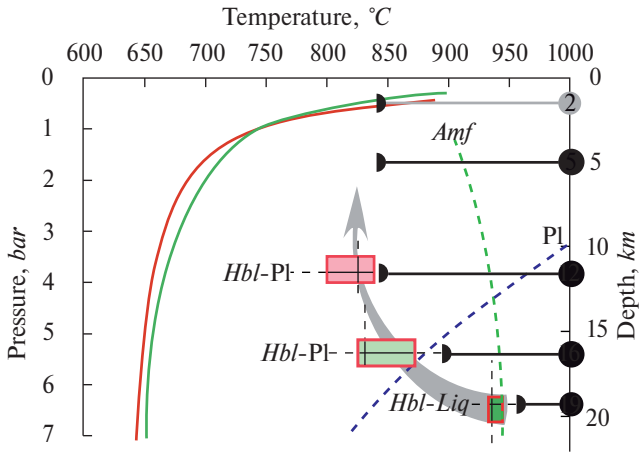

Fig. 8. "Temperature–Pressure–Depth" diagram for quartz monzodiorites of the Viktorinsky complex of the Labaznoe ore field.
Colored lines of water experimental soliduses: red – granodiorite, according to [Schmidt, Thompson, 1996], dark green – tonalite, according to [Bea et al., 2021]; dashed green – amphibole, blue – plagioclase, according to [Schmidt, Thompson, 1996]. Black circles – estimation of pressure and temperature of formation of quartz monzodiorites of the Labaznoe ore field based on their bulk composition according to [Yang, 2017; Duan et al., 2021]. Colored rectangles: dark green – amphibole-melt thermobarometer [Putirka, 2016], light green – central parts, and pink – marginal parts of amphibole and plagioclase paragenesis (temperature [Powell, Holland, 1994], pressure [Mutch, 2016]). Gray arrow – presumed crystallization trend of quartz monzodiorites of the Labaznoe ore field. Red outline – sample LUPb 1_2, blue – sample LUPb 3_4.

in the melt H_2O^{melt} is calculated according to [Ridolfi et al., 2010] and varies from 5.0 to 7.5 wt. %, which corresponds to water-saturated magmas of porphyry deposits [Li et al., 2009].

Based on the obtained thermobarometric estimates, the following sequence of formation of quartz monzodiorites is reconstructed: 1 – amphibole segregation from the melt (Hbl–melt) occurred approximately under subsolidus conditions (T = 940°C, P = 6.45 kbar) at a depth of about 19 km (Fig. 8); 2 – further crystallization of amphibole proceeded together with plagioclase (central parts of grains – 820–870°C, P = 5.4 kbar; marginal parts – 800–850°C, P = 3.5–4.0 kbar) at depths of about 16 and then 12 km; 3 – late magmatic crystallization stage (quartz + feldspar) occurred at a temperature of 840°C and pressure of 2 kbar at a depth of about 5–6 km.

MATERIAL COMPOSITION OF MINERALIZATION AND SECONDARY ALTERATIONS OF ORE-HOSTING ROCKS

At the Labaznoe site, ore mineralization is represented by a sulfide-quartz stockwork and sulfide-quartz veins confined to quartz monzodiorite bodies of the Viktorinsky complex. The area of the stockwork zone is 3.7 km^2 (2.5 × × 1.5 km). Here, in thin stockwork veinlets, gold content up to 0.56 g/t, silver – up to 51.7 g/t, molybdenum – up to 0.3% has been established, according to materials by V.N. Pankov (1990). Within the boundaries of the stockwork zone, later sulfide-quartz veins with gold-silver-polymetallic mineralization are distributed; they form linearly elongated veinlet-vein zones, with thickness from the first few cm to 3.5 m and length up to 750 m. The main part of the veinlet-vein zones is located in the apical parts of the intrusive-dome uplift. According to data from V.N. Shamin et al. (1987) and V.N. Pankov (1990), the maximum gold quantities in the veinlet-vein zones of silver-polymetallic mineralization in hand specimens reach 24 g/t, silver – up to 566 g/t, zinc and lead – 1%, while copper and molybdenum contents were not determined.

In the ore-magmatic system of Labaznoe, we identified hydrothermal stages differing in material composition and sequence of development of the ore veinlet system: 1) magnetite-quartz (Type A, here and below veinlet classification according to [Sillitoe, 2010]) (Fig. 9a); 2) molybdenite-quartz (Type B) (see Fig. 9b, 9c); 3) sulfide-quartz (Type D) (see Fig. 9b, 9c); 4) polymetallic (see Fig 9g, 9d).

The analysis of data obtained by the authors, together with materials from the production report of V.N. Pankov (1990), allows us to conclude that each type of veinlet corresponds to a specific mineralization:

– Pyrite-magnetite-quartz mineral association is the earliest. Magnetite (II) makes up to 50% of the mass of magnetite-quartz veinlets. Quartz in this association is dark gray, microcrystalline, up to 2 mm in size. There are isolated grains of pyrite (I).

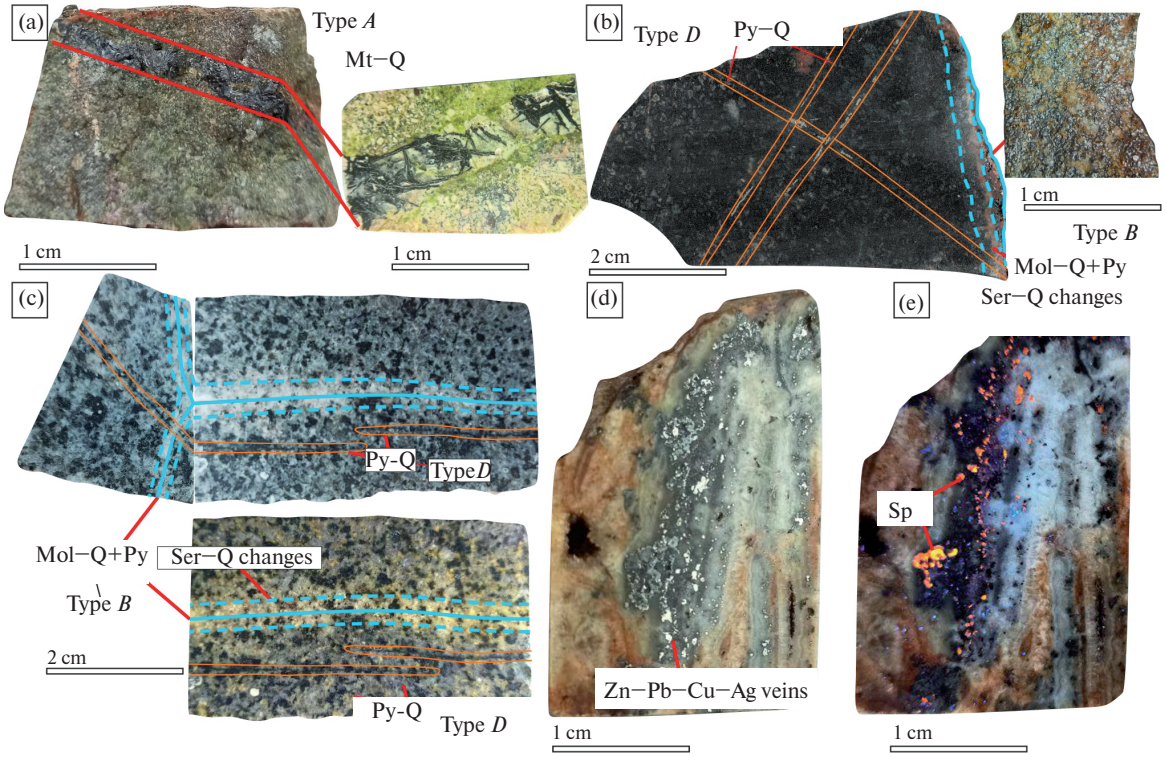

Fig. 9. Varieties of vein formations in rocks of the Labaznoe ore field.
a – magnetite-quartz veinlets in epidotized volcanics of the Kedon series; b – molybdenite-quartz and pyrite-quartz veinlets in andesite-basalts of the Gruntovskaya sequence; c – molybdenite-quartz and pyrite-quartz veinlets in quartz monzodiorites of the Viktorinsky complex (potassium-containing minerals are chemically stained at the bottom); d, e – Zn–Pb–Cu–Ag veins in daylight (d) and ultraviolet (e) light.
Minerals: Q – quartz, Mt – magnetite, Mol – molybdenite, Sp – sphalerite, Py – pyrite, Ser – sericite.

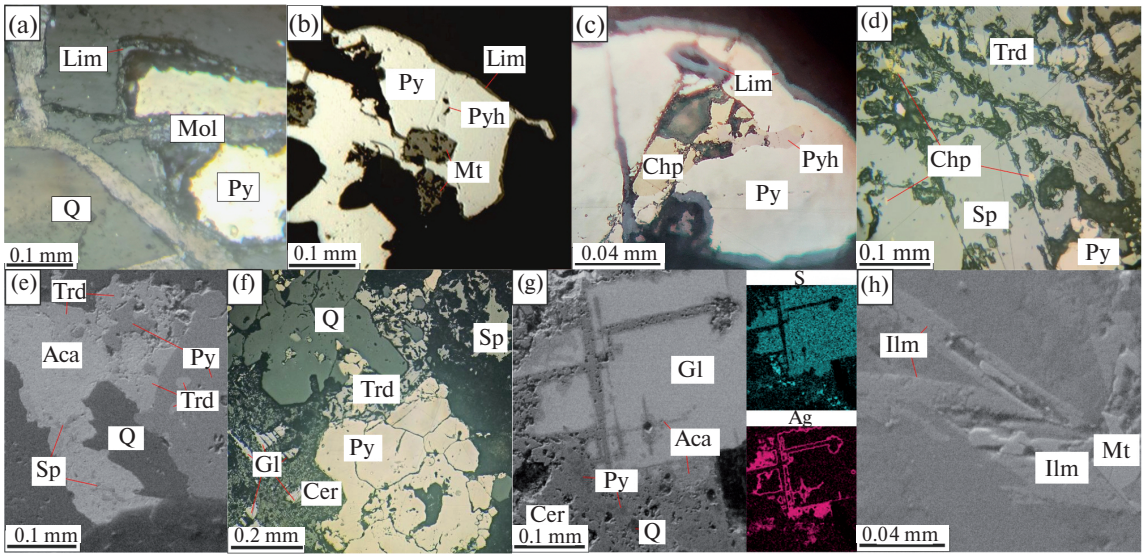

Fig 10. Relationships of ore minerals of the Labaznoe ore field.
a – molybdenite cuts through pyrite in a molybdenite-quartz veinlet; b – magnetite crystals captured by pyrite; c – chalcopyrite and pyrrhotite fill cavities in pyrite, which is covered by a limonite crust; d–g – silver-polymetallic mineralization; h – magnetite-ilmenite intergrowths.
Minerals: Q – quartz; Py – pyrite; Chp – chalcopyrite; Pyh – pyrrhotite; Lim – limonite; Mt – magnetite; Mol – molybdenite; Ilm – ilmenite; Sp – sphalerite; Gl – galena; Cer – cerussite; Aca – acanthite; Trd – tetrahedrite.

Table 3. Results of microprobe analysis of sulfides from the Labaznoe ore field

No.	Sample No.	Total	Weight concentrations, %			Formula coefficients		
Molybdenum-porphyry stage								
Pyrite – $Fe_{1.00}S_{2.00}$								
			S	Fe		S	Fe	
25	210006	99.83	53.27	46.55		2.00	1.00	
52	VL4	100.24	53.59	46.65		2.00	1.00	
136	VL2	99.82	53.56	46.26		2.01	1.00	
31	VL5	100.46	53.61	46.86		2.00	1.00	
As-containing pyrite – $Fe_{1.00}As_{0.01}S_{1.99}$								
			S	Fe	As	S	Fe	As
99	VL5	100.3	53.26	46.54	0.50	1.99	1.00	0.01
Chalcopyrite – $Cu_{0.74}Fe_{0.75}S_{1.51}$								
			S	Fe	Cu	S	Fe	Cu
110	210008	99.98	33.89	27.72	38.37	1.47	0.69	0.84
140	VL7	100.01	35.36	31.72	32.93	1.51	0.78	0.71
172	210008-1	99.79	35.32	30.74	33.73	1.51	0.76	0.73
Pyrrhotite – $Fe_{7.01}S_{7.99}$								
			S	Fe		S	Fe	
100	210008	100.11	40.3	59.81		8.1	6.90	
128	VL2	99.88	38.97	60.92		7.90	7.1	
141	VL7	99.27	38.94	60.34		7.94	7.06	
152	210008-1	99.94	40.36	59.57		8.12	6.88	
Galenite – $Pb_{1.02}S_{0.98}$								
			S	Pb		S	Pb	
43	210005-1	100.2	13.06	87.14		0.99	1.02	
67	210005-1	100.31	13.03	87.27		0.98	1.02	
70	210005-1	100.28	13.39	86.88		1.00	1.00	
67	VL5	99.86	13.1	86.76		0.99	1.01	
Bi-containing galena – $Pb_{0.99}Bi_{0.01}S_{1.00}$								
			S	Pb	Bi	S	Pb	Bi
56	210005-1	98.47	12.86	84.64	0.97	0.99	1.00	0.01
64	210005-1	99.18	13.58	84	1.6	1.01	0.97	0.02
71	210005-1	99.11	13.3	84.7	1.11	1.00	0.99	0.01
Sphalerite – $Zn_{0.96}S_{1.03}$								
			S	Zn	Mn	Fe	Cd	S	Zn	Mn	Fe	Cd
40	VL5	99.24	34.36	64.51	0.37	—	—	1.04	0.96	0.01	—	—

Table 3. *Continued*

No.	Sample No.	Total	Weight concentrations, %					Formula coefficients				
42	VL5	99.04	34.04	64.94	—	—	0.05	1.03	0.97	—	—	—
94	VL5	98.7	33.97	62.25	—	1.05	0.64	1.03	0.93	—	0.02	0.01
Acanthite – $Ag_{1.96}S_{1.04}$												
			S			Ag		S			Ag	
33	VL5	98.29	13.34			84.96		1.04			1.96	
*Ag–Zn–As-tennantite-tetrahedrite **												
			S	Fe	Cu	Zn	As	Ag	Sb	S	Fe	Cu	Zn	As	Ag	Sb
17	VL5	100.02	25.9	0.85	35.15	7.26	8.21	5.22	17.43	13.10	0.25	8.97	1.80	1.78	0.79	2.32
*Ag–Zn-tetrahedrite **																
			S	Fe	Cu	Zn	As	Ag	Sb	S	Fe	Cu	Zn	As	Ag	Sb
39	VL5	98.41	23.91	2.29	27.6	6.53	—	12.41	25.66	13.13	0.72	7.65	1.76	—	2.02	3.71
45	VL5	98.38	23.54	0.36	25.48	6.31	—	15.97	26.73	13.26	0.12	7.24	1.74	—	2.67	3.96
72	VL5	99.36	24.03	—	27.6	6.99	2.33	14.01	24.4	13.15	—	7.62	1.88	0.55	2.28	3.52
98	VL5	99.57	24.87	0.56	30.35	6.81	4.21	10.16	22.61	13.21	0.17	8.13	1.77	0.96	1.60	3.16

Note. Analyst V.Yu. Solov`ev; analysis performed on a Camebax microanalyzer at the North-Eastern Center for Collective Use, NEISRI FEB RAS, Magadan.

* – according to [Mozgova, Tsepin, 1983].

– Pyrite-molybdenite-quartz association is represented by thin veinlets up to several millimeters thick. Relationships where molybdenite flakes cut through pyrite (I) have been observed (Fig. 10a). Quartz is isometric, with isolated inclusions of pyrite (II), which is often replaced by limonite.

– Sulfide-quartz mineral association includes such sulfides as: pyrite (III), chalcopyrite (I), pyrrhotite, arsenopyrite. Pyrite (III) is the most frequently encountered in this association, comprising up to 20% of the veinlet volume. It forms predominantly xenomorphic segregations in quartz, capturing magnetite (I) during formation (see Fig. 10b). Chalcopyrite (I) and pyrrhotite have equilibrium boundaries and are represented by small inclusions up to 0.3 mm in pyrite (III) (see Fig. 10c), rarely in quartz. Chalcopyrite (I) and pyrrhotite are characterized by stoichiometric composition (Table 3). Arsenopyrite is assigned to this association; its description is provided in the report materials of V.N. Pankov (1990), where it appears as large fragmented crystals cemented by non-ore material and chalcopyrite.

– Polymetallic mineralization manifests within the ore occurrence as veinlets and thin quartz veins containing pyrite (IV), sphalerite, galena and products of its hypergene alteration, chalcopyrite (II), acanthite, as well as fahlores. Pyrite (IV) in this association contains an As impurity of up to 0.5%. Chalcopyrite (II) forms small inclusions in sphalerite up to 0.2 mm in size (see Fig. 10d). Sphalerite is deposited as grains up to 3 mm in size, as well as fine disseminations in acanthite (up to 0.05 mm) (see Fig. 10e). Minor impurities include Mn up to 0.37%, Fe up to 1.05%, Cu up to 0.79%, and Cd up to 0.64%. Galena forms relatively large (up to 3 mm) crystals with corroded boundaries, sometimes replaced by anglesite and cerussite, which form a rim around it (see Fig. 10f). Acanthite develops on the surface of galena grains (see Fig. 10g). According to its chemical composition,

galena is stoichiometric (see Table 3), with some grain areas containing Bi impurities up to 1.6%. Acanthite is characterized by two forms of occurrence: a) irregular intergrowths with fahlores and disseminated sphalerite; b) as rims on the surface of galena. The size of segregations reaches 0.5 mm. The chemical composition of acanthite is stoichiometric (see Table 3). In fahlores, there is some variability in composition, characteristic of this type of compounds, but in general, according to the classification of N.N. Mozgovaya [Mozgova, Tsepin, 1983], two groups can be distinguished: 1) Ag–Zn-tetrahedrite; 2) Ag–Zn–As-tennantite-tetrahedrite. The results of microprobe analysis of sulfides are presented in Table 3.

Besides mineralized veinlets, there is disseminated mineralization represented by magnetite (I) (and

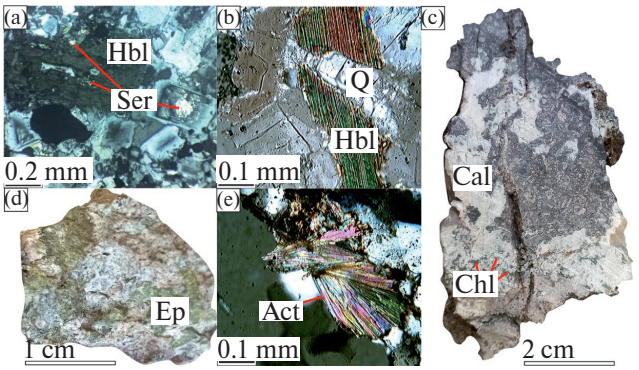

Fig. 11. Secondary alterations of rocks of the Labaznoe ore occurrence.
a, b – sericite-quartz alterations in quartz monzodiorites of the Viktorinsky complex; c, d – actinolite-epidote alterations in quartz veins; e – chlorite-carbonate alterations in crystalloclastic andesite tuff of the Kedon series.
Minerals: Act – actinolite; Ep – epidote; Ser – sericite; Hbl – hornblende; Q – quartz; Cal – calcite; Chl – chlorite.

Table 4. Mineral formation stages of the Labaznoe ore field

Mineral \ Stages	Postmagmatc	Pyrite-magnetite-quartz	Pyrite-molybdenite-quartz	Sulphide-quartz	Polymetallic	Calcite veins	Hypergene stage
Quartz	I	II					
Magnetite							
Ilmenite							
Rutile*							
Hematite							
Pyrite		I	II	III	IV		
Arsenopyrite							
Chalcopyrite				I	II		
Pyrrhotite*							
Molybdenite*							
Sphalerite							
Galenite							
Acanthite*							
Pale ores*							
Calcite							
Limonite*							
Cerussite and Pb oxides*							

Note. Thick lines – common minerals, medium thickness – secondary, thin – rare; * – minerals not previously described at the Labaznoe ore occurrence.

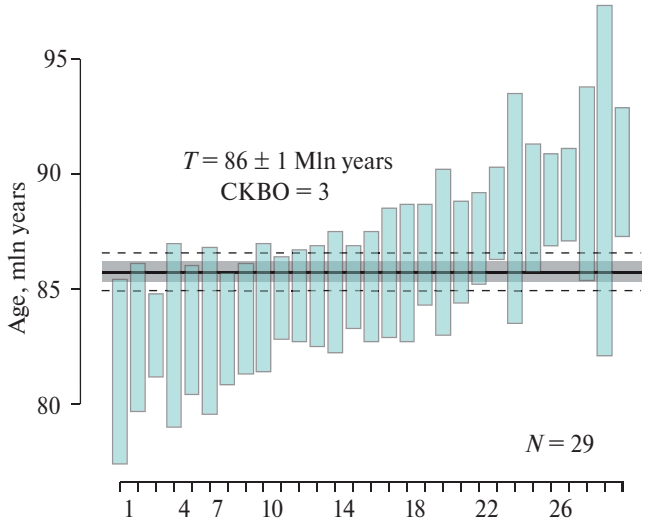

Fig. 12. Weighted average $^{206}Pb/^{238}U$ age diagram of zircons from quartz monzodiorites of the Viktorinsky complex.
Error bars at 2σ level.

its oxidation product – hematite), and to a lesser extent, rutile and ilmenite. Varieties with Ti impurities up to 1.88% have been identified in the composition of magnetite. Ilmenite and rutile are observed as accessory minerals in the host rocks of the Labaznoe ore field; here they form prismatic and irregular crystals up to 0.2 mm in size (see Fig. 10c). In terms of chemical composition, ilmenite belongs to the isomorphic series ilmenite ($FeTiO_3$) – pyrophanite ($MnTiO_3$) with Mn impurities from 7.73 to 8.22%. Rutile contains Fe (up to 13.77%) as an impurity.

In the final stage of hydrothermal activity within the ore field, calcite veinlets are formed. The stages of mineral formation are shown in Table 4 .

The reconstructed sequence of mineral association formation is generally characteristic of Cu–Mo-porphyry systems [Sillitoe, 2010], which indicates the absence of further ore-generating geological events.

Within the ore field, a stockwork zone of secondary metasomatic alterations with zonal arrangement of halos develops in the host volcanics of the Kedon series and granitoids of the Viktorinsky complex. From the central part of the ore field to the peripheral, areas of sericite-quartz (Fig. 11a, 11b), actinolite-epidote-feldspar (see Fig. 11c, 11d), and chlorite-carbonate secondary transformations (see Fig. 11e) are established. The least altered quartz monzodiorites of the Viktorinsky complex are characterized by sericite-quartz alterations.

ON THE AGE OF GRANITOIDS AND MINERALIZATION

Isotopic dating of quartz monzodiorites of the Viktorinsky complex in the central part of the Labaznoe ore occurrence was performed on samples taken from the least altered varieties (sample LBUPb_1, 2) (see Fig. 2). The isolated zircons are transparent, prismatic, idiomorphic, 50–80 μm in size. For 10 grains, 29 measurements of isotopic ratios of the U–Pb system were performed. The obtained results are shown in Fig. 12. The complete table of measured isotopic ratios and ages is available upon request from the authors. For age estimation using $^{206}Pb/^{238}U$ ratio, a correction for common lead ^{207}Pb was made (using the Stacey-Kramers model correction [Stecey, Kramers, 1975]). The obtained weighted mean $^{206}Pb/^{238}U$ age for quartz monzodiorites was 86 ± 1 Ma (Late Cretaceous, Coniacian–Santonian).

Formation of mineralization is the latest thermal event; within the ore field, this process is associated with sericitization of quartz monzodiorites (see Fig. 12a) and host volcanics. To establish the age of the upper boundary of mineralization, K–Ar isotope dating of sericite isolated from the near-vein contact in quartz monzodiorite was carried out (see Fig. 3b). The dating results are as follows: sample number – LUPb_3, 4; dating material – sericite; K = σ – 2.46 ± 0.04%; $^{40}Ar_{rad}$, = 14.20 ± 1.2 ng/g; T ± σ = 82 ± 4 million years. The obtained value, taking into account the error, is close to the estimated time of crystallization of ore-bearing quartz monzodiorites and is interpreted by the authors as the age of the final thermal event within the ore-magmatic system, i.e. as the upper age boundary of mineralization.

DISCUSSION OF RESULTS

The obtained geochronological data fit into the model [Sillitoe, Hedenquist, 2003], according to which granitoid intrusions and

associated molybdenum-porphyry mineralization are considered within the framework of a unified porphyry ore-magmatic system. An example is the Batu Hijau copper-porphyry deposit in Indonesia, for which U-Pb dating results established that the formation interval of ore-bearing multi-phase intrusions does not exceed 0.008 million years [Garwin, 2002]. At the same time, according to R. Sillitoe [2010], the functioning of hydrothermal systems associated with intrusions producing copper-porphyry mineralization depends more on the duration of the intrusive magmatism stage itself.

Thus, a criterion for combining objects of this type can be the close (within the analytical error of the isotopic method) age of magmatism and associated mineralization [Cathles et al., 1997; Cathles, Shannon, 2007; etc.].

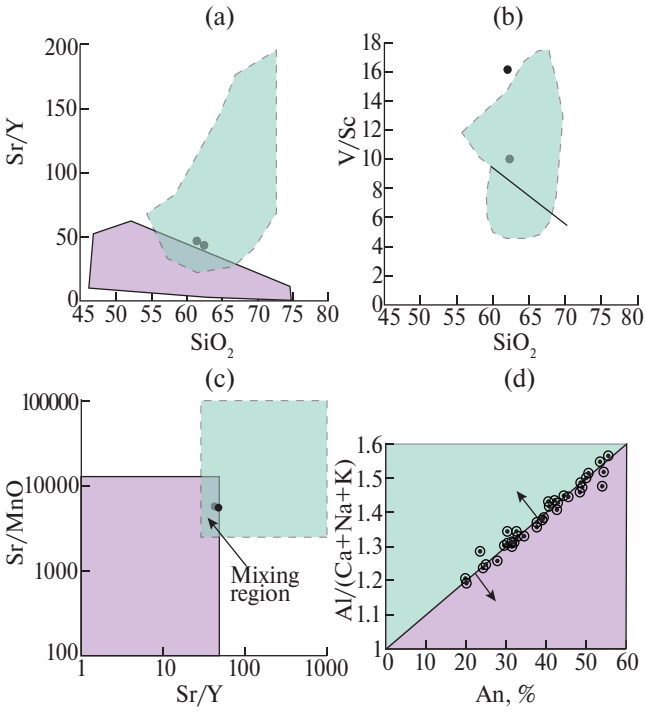

Fig. 13. Composition of monzodiorites from the Labazny ore field (black circles) on discrimination diagrams for identifying potentially ore-bearing intrusions.
a – SiO_2–Sr/Y and b – SiO_2 –V/Sc, after [Loucks, 2014]; c – Sr/Y–Sr/MnO, after [Ahmed et al, 2019]; d – An, %-Al/(Ca + Na + K) in plagioclase, after [Williamson et al., 2016].
Light green color – prospective intrusions for Cu–Au porphyry mineralization, purple color – non-prospective.

The behavior of major and trace elements in the composition of the studied quartz monzodiorites is characteristic of most porphyry systems [Ishihara, 1981; Seedorff et al., 2005]. The presence of so-called adakitic geochemical signatures associated with a high proportion of mantle material in the ore magma is indicative [Li et al., 2009]. Thus, magmatic rocks associated with copper porphyry deposits are characterized by high contents of SiO_2 (⩾56 wt. %), Al_2O_3 (⩾15 wt. %) and Sr (⩾400 ppm) and low contents of Y (⩽18 ppm) and Yb (⩽1.9 ppm) [Defant, Drummond, 1990; Kay, Kay, 1993].

The chemical composition of the Labaznoe quartz monzodiorites generally corresponds to magmas carrying copper-porphyry mineralization – Sr (690–787 ppm), Y (⩽15.8–17 ppm), Yb (1.67––1.9 ppm), Sr/Y (43.7–46.6), and the ratio of a number of chemical elements corresponds to adakitic characteristics (Fig. 13).

In the work of V.Yu. Prokofiev and V.B. Naumov [Prokofiev, Naumov, 2022], based on data from numerous measurements of fluid inclusions in rocks of copper porphyry deposits worldwide (a total of 70 deposits), it was concluded that the composition of fluids separating from melts changes with increasing pressure, in accordance with changes in maximum and average fluid temperatures in various types of porphyry deposits; the authors proposed a hypothetical scheme of the dependence of Cu–Mo–Au porphyry deposit types on the depths of fluid separation from the magmatic melt. Based on these constructions, the crystallization parameters of the monzonitoid melt obtained by us at the Labaznoe ore occurrence (see Fig. 8), as a first approximation, correspond to the molybdenum type of porphyry mineralization.

For the discrimination of potentially ore-bearing (productive for porphyry mineralization) and barren magmas, discrimination diagrams of geochemical parameters calculated from the bulk chemical composition of granitoids can be used. On the diagrams SiO_2–Sr/Y, SiO_2–V/Sc [Loucks, 2014] and Sr/MnO–Sr/Y [Ahmed et al., 2019], the figurative points of the analyzed quartz monzodiorite compositions are located in the areas of granitoids productive for copper-porphyry mineralization (see Fig. 13a, 13b), as well as mixed "productive-unproductive" (see

Fig. 13c), which indicates the prospectivity of the Labaznoe stocks for Cu–Mo–Au porphyry mineralization. The chemical composition of plagioclases is also used to distinguish intrusions by their prospectivity for porphyry mineralization [Williamson et al., 2016]. On the An, %-Al/(Ca+Na+K) diagram, the composition points of plagioclases from quartz monzodiorites are evenly distributed in the areas of prospective (23 analyses) and non-prospective (29 analyses) intrusions for mineralization (see Fig. 13d).

The age values obtained for the Labaznoe ore occurrence from quartz monzodiorites of the Viktorinsky complex (86 ± 1 Ma, U–Pb method on zircon) and sericite isolated from the near-vein contact with monzodiorites (82 ± 4 Ma, K–Ar method) are in good agreement with each other and can serve (considering analytical error) as the time frame for the formation of mineralization.

Overall, the obtained data are comparable with the materials of isotopic dating of granitoids of the Viktorinsky complex [Goryachev et al., 2017; Glukhov et al., 2021; et al.]. Similar age values of granitoid intrusions of the Viktorinsky complex are known for similar objects of copper-porphyry ore-magmatic systems of the Konginsk mineralization zone – copper-molybdenum-porphyry ore occurrence Zakharenko (86.4 ± 1 Ma, U–Pb on zircon, TIMS) and skarn-polymetallic ore occurrence Sedoe/Kustiki (86 ± 1 Ma, U–Pb on zircon, TIMS). The age of mineralization at the Zakharenko ore occurrence, according to ^{40}Ar–^{39}Ar dating of sericite from the host metasomatically altered rhyolites of the Kedon series, was 88.0 ± 1.5 Ma [Glukhov et al., 2021].

In the northern part of the Omolon CT (Namyndykano-Molandzhinsky zone), dates of 82.2 ± 1.0 and 84.6 ± 0.7 million years (U–Pb, SHRIMP-II, [Shatova, Seregin 2023]) were obtained for granitoids of the Victorian complex. The oldest of these, in our opinion, belongs to the granitoids of the Garmandin complex (K_{1-2}, according to LOS-200).

Within the Korkodon-Nayakhan MZ, granitoids of the Nayakhan complex show similar age values – 86–84 ± 1 million years (U–Pb SHRIMP); for the molybdenum-porphyry mineralization of the Ak–Su ore occurrence, associated with the magmatism of the Nayakhan complex, dating of molybdenite showed 84.6 ± 0.5 million years (Re–Os) [Akinin et al., 2019; Sotskaya et al., 2021].

Older, Albian-Cenomanian dates have not yet been identified in the Kongin zone.

CONCLUSIONS

The Labaznoe ore occurrence is confined to an intrusive-dome uplift, in the central part of which stocklike bodies of Late Cretaceous granitoids of the Victorian complex are exposed. Based on the results of thermobarometric estimates of the amphibole–plagioclase pair, the dynamics of polybaric crystallization of quartz monzodiorites from the central part of the Labaznoe ore field was reconstructed. Using mineral thermobarometry methods, the *P-T* conditions of monzonitoid melt crystallization were reconstructed in the following sequence: intratelluric crystallization of amphibole from the melt at a depth of about 19 km (T = 940°C; P = 6.45 kbar), cotectic crystallization of plagioclase and amphibole at depths of about 16 and 12 km (central parts of grains – 820–870°C; P = 5.4 kbar; marginal parts – 800–850°C; P = 3.5–4.0 kbar), final subsolidus crystallization at a depth of about 5–6 km (T = 840°C; P = 2 kbar).

The Labaznoe ore occurrence belongs to the molybdenum-porphyry and polymetallic ore formation with a sequence of mineral paragenesis formation that is classic for a porphyry ore-magmatic system.

A number of ore minerals have been identified: molybdenite, acanthite, fahlores, pyrrhotite, previously undescribed in the Labaznoe ore field.

The attribution of the ore occurrence to the gold-polysulphide mineral type of the gold-silver formation of the Early Devonian-Early Carboniferous metallogenic stage has not been confirmed. The obtained data indicate the possibility of discovering commercial mineralization of the copper-molybdenum-porphyry type in the OChVB.

The close age values of quartz monzodiorites – 86 ± 1 million years, Coniacian–Santonian (U–Pb on zircon), and sericite from sulphide-quartz veinlets in the contact zone of granitoid stocks –

82 ± 4 million years (K-Ar), allow to substantiate the paragenetic relationship between monzonitoids and molybdenum-porphyry mineralization.

The compilation of isotopic dating materials on granitoids of the Viktorinsky complex of the Kongin MZ and associated copper-molybdenum-porphyry mineralization (ore occurrences Labaznoe, Zakharenko, Khrustalnoe, Vechernee, Shlikhovoe) indicates a Late Cretaceous (Coniacian–Campanian) age of the ore-magmatic systems, the functioning of which is associated with the formation of the OChVB.

ACKNOWLEDGEMENTS

The authors express their gratitude for assistance in the work, scientific comments and consultations to Academician of the Russian Academy of Sciences N.A. Goryachev, E.M. Goryacheva, Ph.D in Geology and Minerology, O.T. Sotskaya. The authors express special gratitude to T.A. Kormushin for assistance in conducting field work.

FUNDING

The study of mineralogy and determination of the K–Ar age of muscovite crystallization were carried out with the support of state themes of the NEISRI FEB RAS: "Ore-forming processes and systems in the history of the formation of the main tectonic structures of the Arctic and Pacific continental margins of Northeast Asia" – 121031700301-5, U–Pb age studies were carried out with the support of the research theme "Development of criteria for the ore-bearing capacity of magmatic complexes" – No. 124051600003-4.

CONFLICT OF INTEREST

The authors of this paper declare that they have no conflict of interest.

REFERENCES

1. *Akinin V.V., Miller E.L.* Evolution of calc-alkaline magmas of the Okhotsk-Chukotka volcanic belt // Petrology. 2011. Vol. 19. No. 3. Pp. 249–290.
2. *Akinin V.V., Kolova E.E., Savva N.E., Goryachev N.A., Mamatyusupov V.T., Kuznetsov V.M., Alshevsky A.V., Polzunenkov G.O.* Age of granitoids and associated molybdenum-porphyry mineralization of the Korkodono-Nayakhan zone, Northeast Russia // Bulletin of the North-Eastern Scientific Center FEB RAS. 2019. No. 4. Pp. 3–8.
3. *Akinin V.V., Glukhov A.N., Polzunenkov G.O., Alshevsky A.V., Alekseev D.I.* Age of epithermal gold-silver mineralization at the Kubaka deposit (Omolon cratonic terrane, Northeast Russia): geological and isotope-geochronological (U–Pb, $^{40}Ar/^{39}Ar$) constraints // Pacific Geology. 2020. Vol. 39. No. 1. Pp. 37–47.
4. *Goryachev N.A., Egorov V.N., Savva N.E., Kuznetsov V.M., Fomina M.I., Rozhkov P.Yu.* Geology and metallogeny of Phanerozoic complexes in the southern Omolon massif. Vladivostok: Dalnauka, 2017. 312 p.
5. *Glukhov A.N., Kotov A.B., Priymenko V.V., Salnikova E.B., Ivanova A.A., Plotkina Yu.V., Fedoseenko A.M.* Granitoids of the Kongin magmatic zone of the Omolon massif (Northeast Russia): rock composition, age and geodynamic setting of formation // Geotectonics. 2022. No. 2. Pp. 1–14.
6. *Glukhov A.N., Priymenko V.V., Fomina M.I., Akinin V.V.* Metallogeny of the Kongin zone of the Omolon terrane (Northeast Asia) // Bulletin of the North-Eastern Scientific Center FEB RAS. 2021. No. 2. Pp. 3–16.
7. *Egorov V.N., Sherstobitov P.A., Ermolenko V.G., Grishchenko Sh.G.* Report on GDP-200 for the area of sheets P-57-III, IV, V (new series) South Omolonsky Party. Explanatory note / In 5 books. Magadan: FSUE "Magadangeologia", 2002. 830 p.
8. *Kovalenker V.A., Borisenko A.S., Prokofiev V.Yu., Sotnikov V.I., Borovikov A.A., Plotinskaya O.Yu.* Gold-bearing porphyry-epithermal ore-forming systems: peculiarities of ore mineralogy, fluid regime, factors of large-scale gold concentration // Actual problems of ore formation and metallogeny. Abstracts of the International Meeting. Novosibirsk: Geos, 2006. Pp. 103–104.
9. *Kuznetsov V.M., Akinin V.V., Byakov A.S., Zhulanova I.L., Zheleboglo O.V., Bondarenko S.A., Gusev E.A., Vopilovskaya O.A., Ivanova V.V., Razuvaeva E.I., Suprunenko O.I., Usov A.N.,*

Alekseev D.I., Belikova O.A., Shpikerman E.V. State Geological Map of the Russian Federation, scale 1:1,000,000. Third generation. Verkhoyansk-Kolyma Series. Sheet P-57 (Evensk). Explanatory note. Ministry of Natural Resources of Russia, Rosnedra, FSBI "VSEGEI". St. Petersburg: VSEGEI, 2022. 519 p.

10. *Kuznetsov V.M., Gagiev M.Kh., Dylevsky E.F., Mikhailova V.P., Palymskaya Z.A., Shashurina I.T., Shevchenko V.M., Shpikerman V.I.* Geological map and map of mineral resources of the Kolyma-Omolon region. Scale 1:500 000. Explanatory note. Magadan: SVKNII FEB RAS, 1998. 270 p.

11. *Kuznetsov V.M., Palymskaya Z.A., Shashurina I.T., Mikhailova V.P., Koshkarev V.L.* Metallogenic map of the Kolyma-Omolon region. Scale 1:500 000. Explanatory note. Magadan: SVKNII FEB RAS, 2001. 190 p.

12. *Lychagin P.P., Dylevsky E.F., Likman V.B.* Magmatism of the Omolon median massif // Izv. USSR Academy of Sciences. Geol. ser. 1990. No. 7. Pp. 17–90.

13. *Mozgova N.N., Tsepin A.I.* Fahlores (features of chemical composition and properties). Moscow: Nauka, 1983. 279 p.

14. Petrographic Code of Russia. Magmatic, metamorphic, metasomatic, impact formations. Second edition. St. Petersburg: VSEGEI, 2008. 204 p.

15. *Polzunenkov G.O., Kondratiev M.N.* PETRO: Program for obtaining and processing microphotographs of thin sections using an android smartphone // Bulletin of the North-Eastern Scientific Center FEB RAS. 2023. No. 1. Pp. 28–32.

16. *Sotskaya O.T., Mikhalitsyna T.I., Savva N.E., Goryachev N.A., Mamatyusupov V.T., Semyshev F.I., Malinovsky M.A.* Ore-metasomatic zonation of the Aksu molybdenum-porphyry system (Northeast Asia) // Bulletin of NESC FEB RAS. 2021. No. 3. Pp. 3–17.

17. *Terekhov M.I., Lychagin P.P., Merzlyakov V.M., Zhulanova I.L., Dylevsky E.F., Palymsky B.F.* Explanatory note to the Geological map of the interfluve of Sugoy, Korkodon, Omolon, Oloy, Gizhiga at a scale of 1:500 000. Magadan: SVKNII FESC AS USSR, 1984. 144 p.

18. *Tikhomirov P.L.* Cretaceous continental margin magmatism of Northeast Asia and questions of genesis of the largest Phanerozoic provinces of silicic magmatism. Moscow: GEOS, 2020. 376 p.

19. *Khubanov V.B., Buyantuev M.D., Tsygankov A.A.* U–Pb isotope dating of zircons from PZ_3–MZ magmatic complexes of Transbaikalia using magnetic sector mass spectrometry with laser sampling: determination procedure and comparison with SHRIMP data // Geology and Geophysics. 2016. No. 1. Pp. 241–258.

20. *Shatova N.V., Seregin S.V.* New data on the age of intrusive rocks of the Namyndykan and Viktorinsky complexes in the southern part of the Omolon massif (Magadan region) // Regional Geology and Metallogeny. 2023. No. 93. Pp. 5–27.

21. *Ahmed A., Crawford A.J., Leslie C., Phillips J., Wells T., Garay A., Hood S.B., Cooke D.R.* Assessing copper fertility of intrusive rocks using field portable X-Ray fluorescence (pXRF) data // Geochemistry: Exploration, Environment, Analysis. 2019. Vol. 20.

22. *Bea F., Morales I., Molina J.F., Montero P., Cambeses A.* Zircon stability grids in crustal partial melts: implications for zircon inheritance // Contributions to Mineralogy and Petrology. 2021. Vol. 176.

23. *Boynton W.V.* Geochemistry of rare Earth elements: meteorite studies // Rare Earth Element Geochemistry / Ed. P. Henderson. Netherlands, Amsterdam: Elsevier, 1984. Pp. 63–114.

24. *Cathles L.M., Erend A.H.J., Barrie T.* How long can a hydrothermal system be sustained by a single intrusive event? // Economic Geology. 1997. Vol. 92(7–8). Pp. 766–771.

25. *Cathles L.M., Shannon R.* How potassium silicate alteration suggests the formation of porphyry ore deposits begins with the nearly explosive but barren expulsion of large volumes of mag-matic water // Earth Planet. Sci. Lett. 2007. Vol. 262. Pp. 92–108.

26. *Defant M.J., Drummond M.S.* Derivation of Some Modern Arc Magmas by Melting of Young Subducted Lithosphere // Nature. 1990. Vol. 347. Pp. 662–665.

27. *Donough W.F., Sun S.* Composition of the Earth // Chem. Geol. 1995. Vol. 120. Pp. 223–253

28. *Duan M., Niu Y., Sun P., Chen S., Juanjuan K., Jiyong L., Zhang Y., Hu Y., Shao F.* A simple and robust method for calculating temperatures of granitoid magmas // Mineralogy and Petrology. 2021. Vol. 116. Pp. 93–103.

29. *Frost B.R., Barnes C.G., Collins W.J., Ellis D.J., Frost C.D.* A geochemical classification for granitic rocks // J. Petrol. 2001. Vol. 42. Pp. 2033–2048.

30. *Garwin S.* The geologic setting of intrusion-related hydrothermal systems near the Batu Hijau porphyry copper-gold deposit, Sumbawa // Society of Economic Geologists. 2002. Special Publication 9. Pp. 333–366.

31. *Griffin W.L., Powell W.J., Pearson N.J., O'Reilly S.Y.,* GLITTER: Data reduction software for laser ablation ICP-MS // Mineralogical Association of Canada. 2008. Vol. 40. Pp. 204–207.

32. *Holand T., Blundy J.* Non-ideal interactions in calcic amphiboles and their bearing on amphibole-plagioclase thermometry // Contributions to Mineralogy and Petrology. 1994. Vol. 116. Pp. 433–447.

33. *Hora J.M., Kronz A., Möller-McNett S., Wörner G.* An Excel-based tool for evaluating and visualizing geothermobarometry data // Computers and Geosciences. 2013. Vol. 56. Pp. 178–185.

34. *Ishihara S.* The granitoid series and mineralization // Economic geology. 1981. Vol. 75. Pp. 458–484.

35. *Jarosewich E., Nelson J.A., Norbers J.A.* Reference samples for electron microprobe analysis // Geostandards Newsletter. 1980. Vol. 4. Pp. 43–47.

36. *Kay R.W., Kay S.M.* Delamination and delamination magmatism // Tectonophysics. 1993. Vol. 219. Pp. 177–189.

37. *Laurence N. Warr.* IMA-CNMNC approved mineral symbols // Mineralogical Magazine. 2021. Vol. 85(3). Pp. 291–320.

38. *Leake B.E., Woolley A.R., Arps C.E., Birch W.D., Gilbert M.C., Grice J.D., Hawthorne F.C., Kato A., Kisch H.J., Krivovichev V.G.* Nomenclature of amphiboles: report of the subcommittee on amphiboles of the International mineralogical association commission on new minerals and mineral names // Mineral. magazine. 1997. Vol. 61. No. 2. Pp. 295–321.

39. *Li L.X., Song Q.H., Wang D.H., Wang C.H., Qu W.J., Wang Z.G., Bi S.Y., Yu C.* Re-Os isotopic dating of molybdenite from the Fuanpu molybdenum deposit of Jilin Province and discussion on its metallogenesis // Rock and mineral analysis. 2009. Vol. 28. Pp. 283–287.

40. *Loucks R.R.* Distinctive composition of copper-ore-forming arcmagmas // Australian Journal of Earth Sciences. 2014. Vol. 61. Pp. 5–16.

41. *Mutch E.J.F., Blundy J.D., Tattitch B.C., Cooper F.J., Brooker R.A.* An experimental study of amphibole stability in low-pressure granitic magmas and a revised Al-in-hornblende geobarometer // Contributions to Mineralogy and Petrology. 2016. Vol. 171.

42. *Pearce J.A., Harris N.B., Tindle A.G.* Trace elements discrimination diagrams for the tectonic interpretation of granitic rocks // Journal of Petrology. 1984. Vol. 25. Pp. 956–983.

43. *Peccerillo R., Taylor S.R.* Geochemistry of Eocene calc-alkaline volcanic rocks from the Kastamonu area, northern Turkey // Contributions to Mineralogy and Petrology. 1976. Vol. 58. Pp. 63–81.

44. *Powell R., Holland T.J.B.* Optimal geothermometryand geobarometry // American Mineralogist. 1994. Vol. 79. Pp. 120–133.

45. *Prokofiev V.Y., Naumov V.B.* Ranges of physical parameters and geochemical features of mineralizing fluids at porphyry deposits of various types of the Cu–Mo–Au system: Evidence from fluid inclusions data // Minerals. 2022. Vol. 12(5). 529. Pp. 1–23.

46. *Putirka K.* Amphibole thermometers and barometers for igneous systems and some implications for eruption mechanisms of felsic magmas at arc volcanoes // American Mineralogist. 2016. Vol. 101. Pp. 841–858.

47. *Ridolfi F., Renzulli A., Puerini M.* Stability and chemical equilibrium of amphibole in calc-alkaline magmas: an overview, new thermobarometric formulations and application to subduction-related volcanoes // Contributions to Mineralogy and Petrology. 2010. Vol. 160. Pp. 45–66.

48. *Seedorff E., Dilles J.H., Proffett J.M., Einaudi M.T., Zurcher L., Stavast W.J.A., Johnson D.A., Barton M.D.* Porphyry deposits: Characteristics and origin of hypogene features // Economic geology. 2005. Vol. 100. Pp. 251–298.

49. *Schmidt M.W., Thompson A.B.* Epidote in calc-alkaline magmas: An experimental study of stability, phase relationships, and the role of epidote in magmatic evolution // American Mineralogist. 1996. Vol. 81. Pp. 462–474.

50. *Sillitoe R.H.* Porphyry copper system // Economic geology. 2010. Vol. 105. Pp. 3–41.

51. *Sillitoe R.H., Hedenquist J.W.* Linkages between volcanotectonic setting, ore-fluid composition and

epitermal precious-metals deposits // Economic geology. 2003. Special Publication 10. Pp. 315–343.

52. *Steiger R.H., Jager E.* Subcommission on geochronology: Convention on the use of decay constants in geo- and cosmochronology // Earth Planet. Sci. Lett. 1977. Vol. 36. Pp. 359–362.

53. *Stacey J.S., Kramers I.D.* Approximation of terrestrial lead isotope evolution by a two stage model // Earth Planet. Sci. Lett. 1975. Vol. 26. Pp. 207–221.

54. *Van Achterbergh E., Ryan C.G., Jackson S.E., Griffin W.L.* Data reduction software for LA–ICP–MS: appendix // Mineralogical Association of Canada. 2001. Vol. 29. Pp. 239–243.

55. *Vermeesch P.* IsoplotR: a free and open toolbox for geochronology // Geoscience Frontiers. 2018. Vol. 9. Pp. 1479–1493.

56. *Wiedenbeck M., Alle´ P., Corfu F., Griffin W.L., Meier M., Oberli F., Von Quadt A., Roddick J.C., Spiegel W.* Three natural zircon standards for U–Th–Pb, Lu–Hf, trace element and REE analyses // Geostandard Newsletter. 1995. Vol. 19. Pp. 1–23.

57. *Williams I. S.* U–Th–Pb Geochronology by Ion Microprobe // Reviews in Economic Geology. 1998. Vol. 7. Pp. 1–35.

58. *Williamson B. J.; Herrington R. J.; Morris A.* Porphyry copper enrichment linked to excess aluminum in plagioclase // Nature Geosci. 2016. Vol. 9. Pp. 237–241.

59. *Yang X.* Estimation of crystallization pressure of granite intrusions // Lithos. 2017. Vol. 286–287. Pp. 324–329.